ANTICANCER RESEARCH *45*: 5287-5297 (2025)
doi: 10.21873/anticanres.17868

Inhibition of Small-cell Lung Cancer Angiogenesis by Irinotecan Metronomic Chemotherapy and Irinotecan Plus Everolimus

YOSHIHIRO AMANO, RYOSUKE TANINO, RONG SUN, YUKARI TSUBATA, TAKESHI ISOBE and TAMIO OKIMOTO

Department of Internal Medicine, Division of Medical Oncology & Respiratory Medicine,
Shimane University Faculty of Medicine, Izumo, Japan

Abstract

Background/Aim: Few drugs are effective against small-cell lung cancer (SCLC) after second-line treatment, and suppressing rapid angiogenesis in tumor tissues has been considered an option. Metronomic chemotherapy can suppress angiogenesis while reducing toxicity, and irinotecan has antitumor effects against SCLC. Everolimus is an mTOR inhibitor that inhibits angiogenesis. This study investigated the inhibition of SCLC angiogenesis by irinotecan (CPT-11) metronomic chemotherapy and irinotecan plus everolimus.

Materials and Methods: Human SCLC cell lines N417, H82, and H187 were used. Cell viability was measured using the WST-8 assay. *VEGFA* gene expression was quantified using reverse transcription quantitative PCR (RT-qPCR). An orthotopic human SCLC xenograft model was used to assess cytotoxicity and angiogenesis after intravenous administration of irinotecan and everolimus. Immunohistochemistry for CD31 was performed to detect blood vessels in the tumor. Terminal transferase dUTP nick end labeling (TUNEL) staining was performed for in situ detection of apoptosis.

Results: CPT-11 and everolimus alone inhibited the growth of SCLC cells *in vitro.* The combination of everolimus and irinotecan did not alter the cytotoxic effects of CPT-11. Irinotecan and everolimus did not induce *VEGFA* expression. Immunohistochemistry revealed that the microvessel density upon daily CPT-11 and weekly irinotecan plus everolimus was comparable to that of weekly CPT-11 (positive control). Daily administration of CPT-11 inhibited vascular angiogenesis, whereas the concomitant administration of CPT-11 and everolimus did not. In contrast, the combination of CPT-11 and everolimus induced tumor apoptosis.

Conclusion: Daily administration of CPT-11 may have significant antitumor effects based on its anti-angiogenic effects. Daily administration of CPT-11 may be a novel second-line option for SCLC.

Keywords: Small cell lung cancer, anti-angiogenesis, orthotopic models.

Tamio Okimoto, Department of Internal Medicine, Division of Medical Oncology & Respiratory Medicine, Shimane University Faculty of Medicine, 89-1 Enya-cho, Izumo-shi, Shimane 693-8501, Japan. Tel/Fax: +81 853202581, +81 853202581, e-mail: okimoto@med.shimane-u.ac.jp

Received September 11, 2025 | Revised September 27, 2025 | Accepted September 29, 2025

Introduction

Small-cell lung cancer (SCLC) represents approximately 10-15% of all lung cancers and is classified as a neuroendocrine tumor by the World Health Organization (WHO) (1-3). At the time of diagnosis, nearly 70% of patients present with distant metastases, reflecting its highly aggressive nature. While recent advances in molecular targeted therapies and immunotherapy have improved survival in non-small cell lung cancer (NSCLC) (4, 5), comparable progress in SCLC has been limited. Immune checkpoint inhibitors have shown modest benefit, and no targeted therapies have been approved for SCLC. Moreover, no biomarker has been established for the prediction of chemo-immunotherapy (6). Thus, there is a pressing need for novel therapeutic strategies.

Metronomic chemotherapy (MCT), defined as the frequent administration of low-dose chemotherapy without extended drug-free intervals, differs from conventional maximum tolerated dose regimens (7). MCT has been associated with reduced toxicity, decreased risk of drug resistance, and modulation of the tumor microenvironment through immunological and anti-angiogenic effects (8). Irinotecan (CPT-11), a topoisomerase I inhibitor widely used in SCLC, has shown promise in metronomic schedules for other malignancies, such as colorectal cancer and sarcoma (9, 10). However, data on its role in SCLC remain scarce.

Given that angiogenesis is essential for SCLC progression and vascular endothelial growth factor (VEGF) expression correlates with poor prognosis (11, 12), angiogenesis represents a rational therapeutic target. Although VEGF inhibition with bevacizumab was successful in NSCLC, it failed to demonstrate benefit in combination with cisplatin/etoposide in SCLC (13, 14). Everolimus (EVE), an mTOR inhibitor, exerts antitumor effects by modulating the STAT3/HIF-1α/VEGF signaling axis and reducing angiogenesis (15). Although clinical trials of EVE in SCLC have yielded modest efficacy (16), a clinical trial suggests potential synergy when combined with other agents (17).

In this context, we investigated the therapeutic potential of combining metronomic CPT-11 with EVE, focusing on their anti-angiogenic effects in an orthotopic mouse model of SCLC.

Materials and Methods

Cell culture and reagents. The human lung SCLC cell lines H82 (ATCC, Manassas, VA, USA. HTB-175; RRID: CVCL_1591), H187 (ATCC, Manassas, VA, USA; CRL-5804; RRID: CVCL_1501), and N417 (ATCC, Manassas, VA, USA; RRID: CVCL_1602) were used. Cell line authentication was performed for N417 cells by short tandem repeat profiling using the JCRB Cell Bank database (Osaka, Japan). The cells were cultured in RPMI 1640 medium (Fujifilm Wako Pure Chemical Corporation, Osaka, Japan) and supplemented with 10% FBS and 50 μg/ml gentamicin (Nacalai Tesque, Kyoto, Japan) at 37˚C in a humidified 5% CO_2 incubator. SN38 and CPT-11 hydrochloride trihydrate were obtained from Yakult Honsha (Tokyo, Japan). EVE and imatinib mesylate (IMA) were purchased from Selleck Chemicals (Houston, TX, USA). The drugs were diluted with dimethyl sulfoxide (DMSO, Fujifilm Wako Pure Chemical Corporation).

Cell viability assay. Cell viability was determined using a 4-(3-(2-methoxy-4-nitrophenyl)-2-(4-nitrophenyl)-2 H-5-tetrazolio)-l, 3-benzene disulfonate sodium salt (WST-8) assay and a Cell Counting Kit-8 (CCK-8; Dojindo Laboratories, Kumamoto, Japan). Cells were seeded in a 96-well plate at a density of 5000 cells/well and cultured with the indicated doses of the drug-containing medium. Absorbance was measured using a Sunrise R microplate reader (Tecan Group, Männedorf, Switzerland) at 450 nm (reference wavelength: 630 nm). The absorbance of the blank wells was subtracted from each absorbance value. The absorbance of each well was expressed as a percentage of the growth relative to the untreated cells to determine the relative cell viability percentage.

Reverse-transcription quantitative polymerase chain reaction (RT-qPCR). Total RNA was extracted from cultured cells in a 6-well plate using an RNeasy Mini Kit (Qiagen,

Hilden, Germany). RNA was reverse-transcribed to cDNA using the ReverTra Ace qPCR RT Master Mix with gDNA Remover (Toyobo, Osaka, Japan) according to the manufacturer's instructions. The primers, cDNA, and KOD SYBR qPCR Mix (Toyobo) were mixed, and qPCR was performed using a Thermal Cycler Dice Real Time System II (TaKaRa Bio, Kusatsu, Shiga, Japan). The sequences of the primers used are as follows: 5'- GATCTCTCACCAGG AAAGACTGATAC-3' and 5- CAGAGTCTCCTCTTCCTTCAT TTCAG-3' for VEGFA; 5'- GCACCGTCAAGGCTGAGAAC-3' and 5'-TGGTGAAGACGCCAGTGGA-3' for GAPDH. GAPDH was used as the normalization standard for relative expression. The qPCR was performed with a predenaturation step of 98˚C for 2 min and 40 cycles of 98˚C for 10 s, 60˚C for 10 s, and 68˚C for 30 s.

Orthotopic mouse models. The Committee for Animal Experimentation of Shimane University, Shimane, Japan (no IZ30-67) approved all animal experimental protocols. The protocol met the ethical standards required by the law and the guidelines for animal experiments in Japan. Five-week-old female BALB/cA-nu/nu mice aged 5 weeks were purchased from CLEA Japan (Tokyo, Japan). N417 cells (2×10^6) were injected subcutaneously into the left lungs of 7-week-old mice, according to a previous study (18).

First study. First, we experimented to confirm the tumor-reducing effects of each agent. We transplanted 1.0×10^6 cells/100μl (50 μl RPMI + 50 μl Matrigel) into the left lung of each mouse. The mice were randomly assigned to the following four groups (six mice per group) three weeks after the N417 injection: control (Control) administered vehicle, weekly CPT-11 (wCPT) administered at a dose of 25 mg/kg per week for three weeks, daily CPT-11 (dCPT) administered at a dose of 5 mg/kg on weekdays for three weeks, and Everolimus (EVE) administered at a dose of 5 mg/kg per week for three weeks. All the agents were administered intraperitoneally. The vehicle was administered intraperitoneally on weekdays to reduce intergroup bias due to invasiveness (Figure 1A). The experiment was repeated once.

Second study. We transplanted 7.5×10^5 cells/75 μl (37.5 μl RPMI + 37.5 μl Matrigel) into the left lung of each mouse. The mice were randomly assigned to the following four groups (six mice per group): control (Control) administered vehicle, weekly CPT-11 (wCPT) administered at 25 mg/kg per week for two weeks, daily CPT-11 (dCPT) administered at 5 mg/kg on weekdays for two weeks, CPT-11 plus EVE (wCPT+EVE) administered at 25 mg/kg per week for two weeks, and EVE administered at 5 mg/kg per week for 2 weeks. CPT-11 was dissolved in phosphate-buffered saline (PBS) and administered intraperitoneally. EVE, dissolved in 30% propylene glycol, and 5% Tween 80, was administered orally. The mice were sacrificed four days after the administration of each treatment (Figure 1B). This experiment was repeated once. The same dose intensity was maintained in both studies.

Immunohistochemistry. Tumor tissues were formalin-fixed, paraffin-embedded, and sectioned (4 μm). Deparaffinization and antigen retrieval (CC1, Roche, Basel, Switzerland) were performed using a Ventana Benchmark XT (Roche). Slides were incubated with anti-CD31 antibody (1:100, Cell Signaling Technology, Danvers, MA, USA; RRID: AB_2799574) at 37˚C for 30 min, followed by SignalStain Boost IHC Detection Reagent (#8114, Cell Signaling Technology) for 30 min at room temperature. Detection was achieved with UltraView Universal DAB (Roche), and counterstaining was performed with Hematoxylin II (Roche). Images were captured with a BX53 microscope (Olympus, Tokyo, Japan). Quantification of CD31-positive area was performed using ImageJ (NIH, Bethesda, MD, USA). Background subtraction (rolling ball radius=50), color deconvolution ([H DAB] vector), and thresholding (Otsu for hematoxylin, Yen for DAB) were applied. The ratio of DAB-positive to hematoxylin-positive area was defined as staining intensity.

Immunofluorescence and DNA fragment staining. Frozen tumor tissue slices (10 μm) were placed on a glass slide. The slice was fixed with methanol at –20˚C for 10 min and

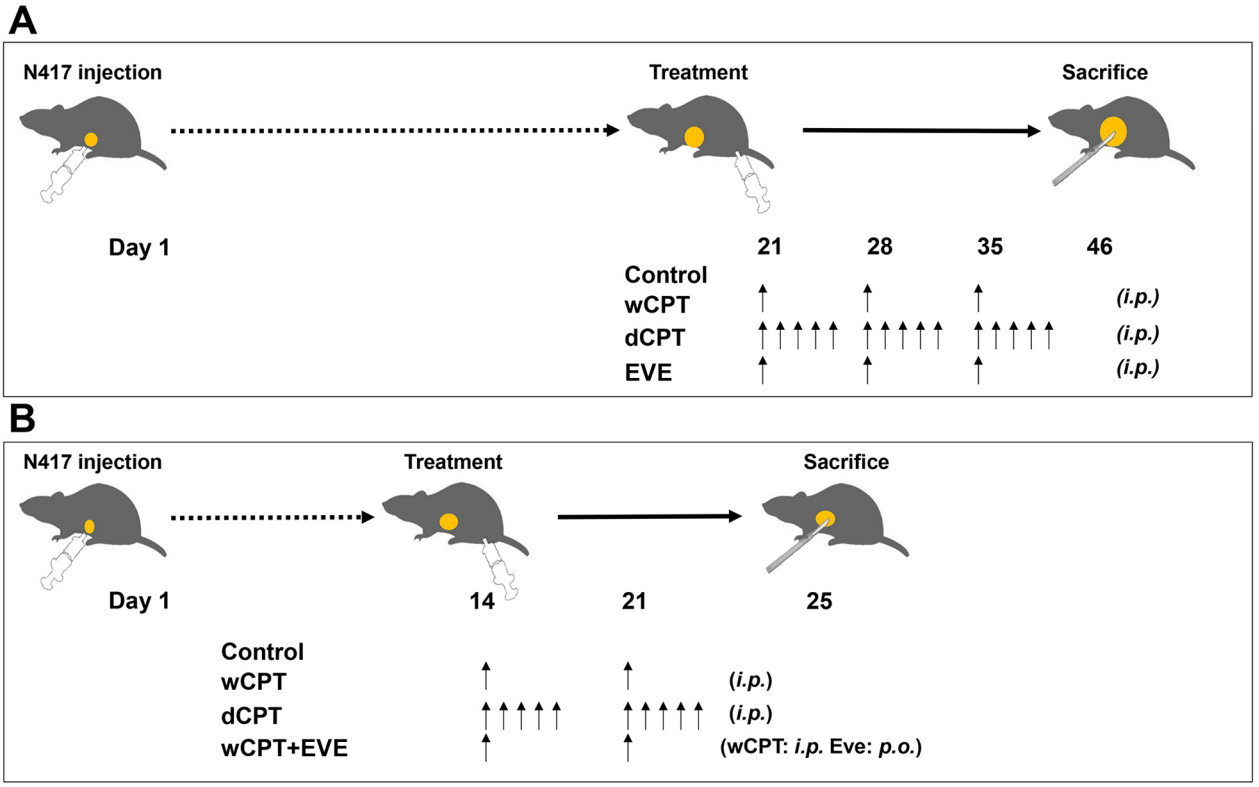

Figure 1. *Schema of the orthotopic mouse model. (A) First study. The control group was administered vehicle; the weekly irinotecan (CPT-11) group (wCPT) was administered CPT-11 at 25 mg/kg weekly for three weeks. The daily CPT-11 group (dCPT) was administered CPT-11 at 5 mg/kg on weekdays for three weeks. The weekly CPT-11 plus everolimus (EVE) group (wCPT11+EVE) was administered CPT-11 at 25 mg/kg per week and EVE at 5 mg/kg per week for three weeks. CPT-11 and EVE were administered through an intraperitoneal injection. The mice were sacrificed on day 46. The number of mice in each group was six. (B) The second study. The control group was administered vehicle; the wCPT group was administered CPT-11 at 25 mg/kg per week for two weeks; the daily dCPT group was administered CPT-11 at 5 mg/kg on weekdays for two weeks; and the wCPT11+EVE group was administered CPT-11 at 25 mg/kg per week and EVE at 5 mg/kg per week for 2 weeks. CPT-11 was administered through an intraperitoneal injection. EVE was administered per os. Mice were sacrificed on day 46. The number of mice in each group was six.*

washed twice with ice-cold PBS. The slice was blocked with 0.3% Triton X-100 (Merck, Darmstadt, Germany) and 10% Blocker BSA in PBS (Thermo Fisher Scientific, Waltham, MA, USA) for 60 min at 20-25˚C. The slice was incubated overnight with anti-CD31 antibody (1:100, 553370, BD Biosciences, Franklin Lakes, NJ, USA; RRID: AB_394816) diluted in 10% Blocker BSA (Thermo Fisher Scientific) in PBS at 4˚C. The slice was washed twice with PBS and incubated with anti-rat IgG2a antibody conjugated with Alexa Fluor 488 (ab172332, Abcam, Cambridge, UK; RRID: AB_2893134) for 60 min at 20-25˚C. Terminal deoxynucleotidyl transferase dUTP nick-end labeling (TUNEL) staining was performed using the Click-iT Plus TUNEL Assay and Alexa Fluor 594 (Thermo Fisher Scientific), according to the manufacturer's protocol for tissue sections without deparaffinization. The slice was washed with PBS twice and mounted with ProLong Diamond Antifade Mountant with DAPI (Thermo Fisher Scientific). Fluorescent images were obtained using a confocal laser scanning microscope FV1000D (Olympus).

Statistical analysis. Significant differences between the treatment outcomes were evaluated using the Student's unpaired two-tailed *t*-test. Differences between more than two groups were assessed using one-way ANOVA and a

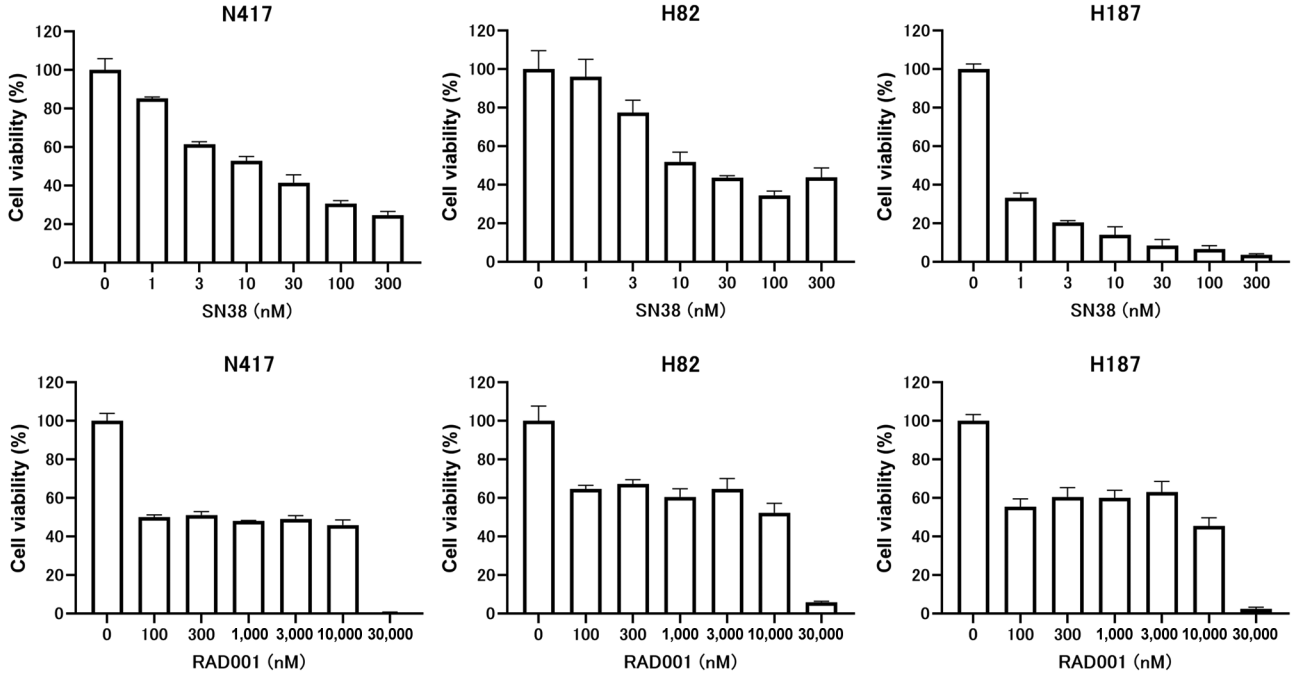

Figure 2. C*ytotoxicity of SN38 and EVE for small-cell lung cancer cell lines. Each cell line was treated for 48 h at the indicated concentrations. Data are presented as means (SD), N=3. Each p-value was <0.0001. The* IC_{50} *values for SN38 were 22.9 nM (N417), 23.5 nM (H82), and <1 nM (H187).*

post-hoc test. Statistical significance was set at $p<0.05$. All data were analyzed using GraphPad Prism version 9.3.1 for Windows (GraphPad Software, La Jolla, CA, USA).

Results

Cytotoxicity of drugs for small-cell lung cancer cell lines. We evaluated the cytotoxicity of SN38 and EVE using the WST-8 assay. The N417, H82, and H187 cell lines were used. The cells were exposed to 0-300 nM of SN38 and 0-30,000 nM EVE for 48 h (Figure 2). SN38 exhibited concentration-dependent cytotoxicity in all the cell lines. The IC_{50} values of SN38 were 22.9 nM, 23.5 nM, and <1 nM for N417, H82, and H187, respectively. Among the cell lines tested, H187 showed the highest sensitivity to SN38. In contrast, EVE showed no concentration-dependent cytotoxicity, with cell viability ranging from 49.9% to 64.7% at 100 nM (Figure 2).

Next, we investigated the cytotoxicity of EVE with or without SN38 against N417 cells. The concentration of EVE ranged from 0-300 nM, whereas that of SN38 was maintained at 3 nM. Cells treated with EVE+SN38 showed sparse growth in the micrograph, but the WST-8 assay did not show any enhancement or mutual inhibition of cytotoxicity (Figure 3).

Expression intensity of VEGFA in small-cell lung cancer cell lines. The WST-8 assay results indicated that 10 nM SN38 and 300 nM EVE effectively inhibited the cell growth (Figure 2). N417 and H82 cell lines were exposed to either CPT-11 at 10 nM or EVE at 300 nM for 24 h. Subsequently, VEGFA expression was measured using RT-qPCR. The VEGFA mRNA expression levels were normalized to those of GAPDH (1). Although there were no significant differences in VEGFA expression between the treatment groups, VEGFA expression was lower in both EVE-treated cells compared to untreated and SN38-treated cells. The VEGFA expression levels in the N417 cells were 0.00227, 0.00291, and 0.00202 for the untreated control, SN38, and

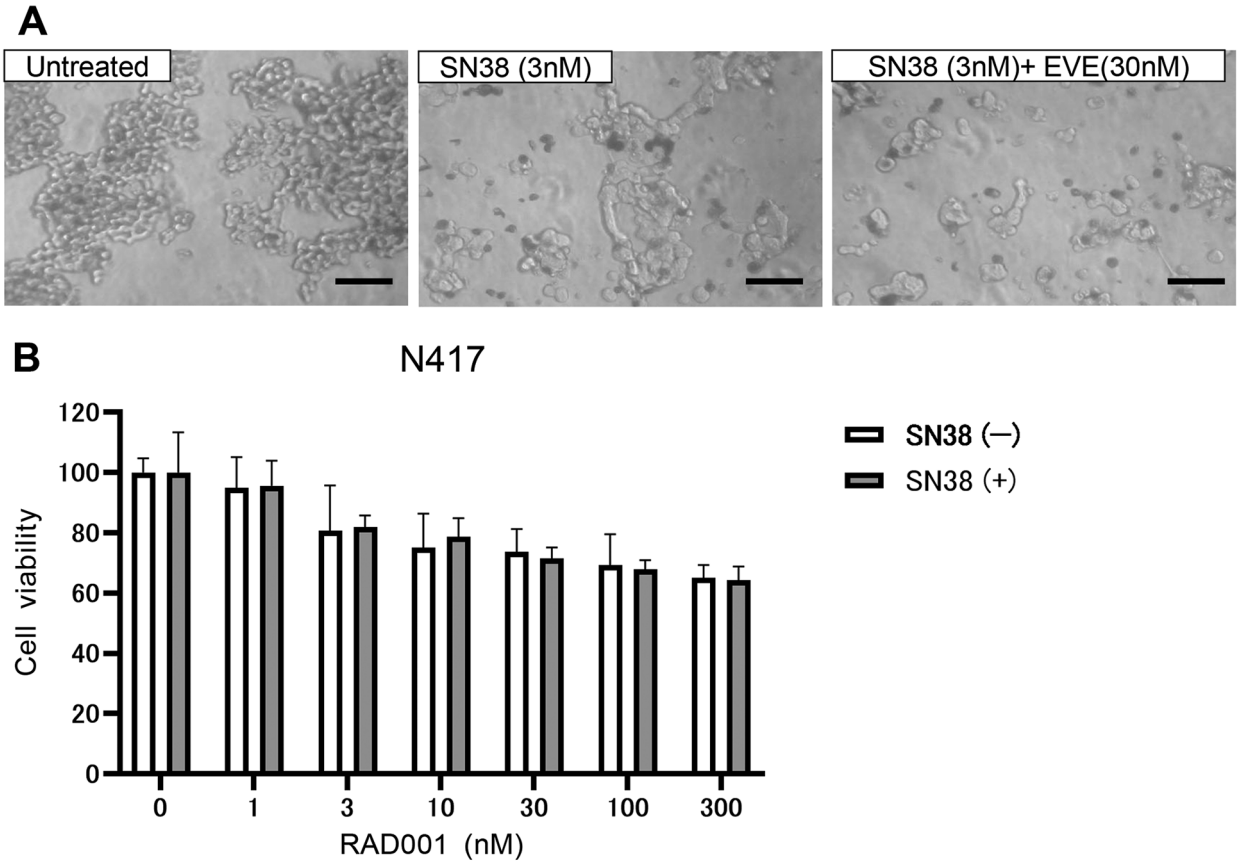

Figure 3. *Effect of the combined use of SN38 and EVE on N417 cells. (A) Micrograph of N417 cells exposed for 48 hours (N=3). (B) N417 cell viability with varying EVE concentrations. The concentration of SN38 was fixed at 3 nM (N=3). Each p-value was >0.999. Scale bar indicates 20 μm.*

EVE groups, respectively. In H82 cells, the VEGFA expression levels in the untreated control, SN38, and EVE groups were 0.00721, 0.00781, and 0.00557, respectively (Figure 4).

Antitumor effects of CPT-11 and EVE in orthotopic mouse models. This study used the N417 cell line because it is suitable for developing an orthotopic mouse model of small-cell lung cancer. In the first experiment, mice in the control, wCPT-11, dCPT-11, and EVE groups were sacrificed 46 days after N417 injection. A large mass in the injected left lung showed progressive local engraftment (Figure 5A).

Comparison of the left lung weights revealed that the dCPT-11 group exhibited the most significant reduction in tumor size, which was significantly different from that of the control group (Control: 1.085±0.118 g, dCPT-11: 0.391±0.162 g; n=6 for each group; p=0.044). The wCPT-11 and EVE groups also showed a trend toward tumor reduction (Figure 5B). One mouse in the control group died on day 35, and another mouse in the EVE group died on day 21.

The first study showed the antitumor effects of anticancer drugs, but death occurred because of the large tumor volume and long treatment duration. The second study evaluated the effect of anticancer drugs on tumor neovascularization while the tumor remained intact. This study reduced the number of transplanted cells to 75%, and the animals were sacrificed earlier. Mice in the control, wCPT-11, dCPT-11, and wCPT-11+EVE groups received N417 injections 25 days before sacrifice. There were no significant differences in body weight among the groups during the treatment period (Control/wCPT-11/

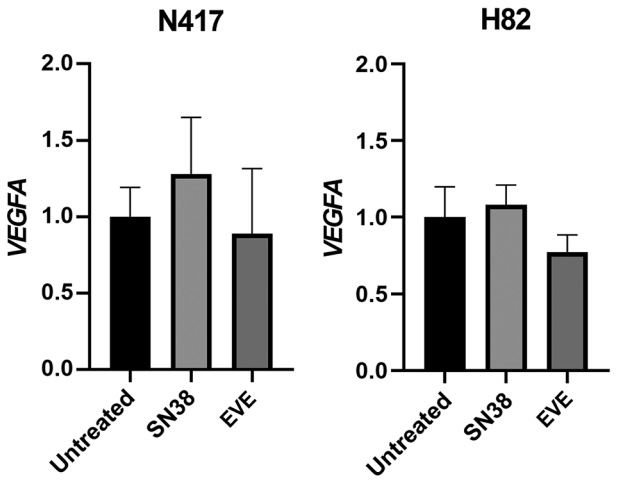

Figure 4. *Effects of VEGFA expression inhibition by SN38 and everolimus on small-cell lung cancer cell lines. The mRNA expression of VEGFA was calculated using GAPDH as 1. Data are means (standard deviation), N=3. Each p-value was >0.2.*

dCPT-11/wCPT-11+EVE=21.7 g/21.5 g/21.6 g/21.7 g). No differences were observed in the weights of the sacrificed lungs (Ctrl/wCPT-11/dCPT-11/wCPT-11+EVE=0.186 g/0.180 g/0.173 g/0.182 g) (Figure 6A-C). In the second study, no deaths occurred, and the specimens were collected in a manner that fulfilled the study objectives.

Tumor vessels were evaluated using CD31 immunostaining. In the macrographs, the wCPT-11, dCPT-11, and wCPT-11+EVE groups, particularly the dCPT-11 group, appeared to have fewer neovessels than the control group (Figure 6D). The intensity of CD31 staining of the tumors was quantified using the ImageJ software (Figure 6E). While no significant differences were found following quantification (N=2), there was less variability in the wCPT-11+EVE group. When the density of neovessels in the control group was set to 1, the densities of the other groups were as follows: wCPT-11, 0.656; dCPT-11, 0.674; and wCPT-11+EVE, 0.639. The addition of EVE to CPT-11 did not decrease neovessel formation (Figure 6E).

Tumor apoptosis analysis. TUNEL staining was performed to assess apoptosis in tumor tissues. CD31 immunofluorescence confirmed vascular structures, while TUNEL identified apoptotic cells. Apoptosis was not

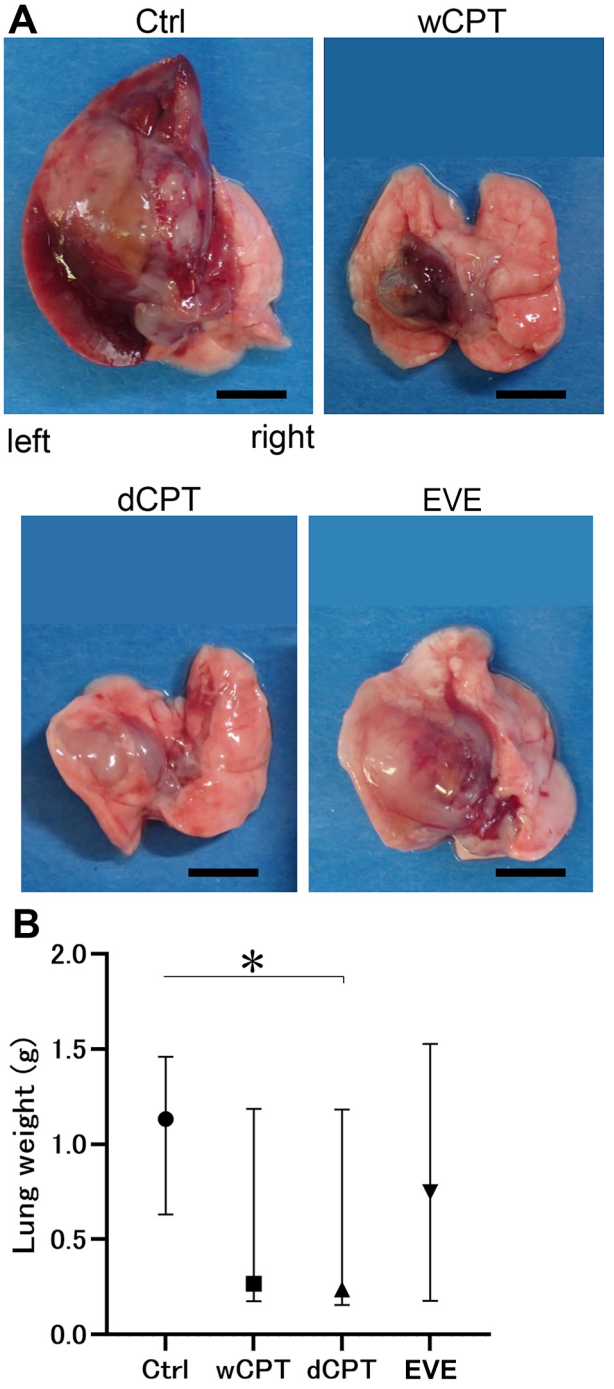

Figure 5. *Evaluation of drug efficacy using orthotopic mouse models in the first study. (A) The photographs show typical examples of each group. Scale bar indicates 5 mm. (B) Left lung weights, including tumor, in the first study. There was a significant difference between the daily CPT-11 group and controls (p=0.044). N=6 for Control, dCPT-11, and wCPT-11 groups, N=4 for EVE.*

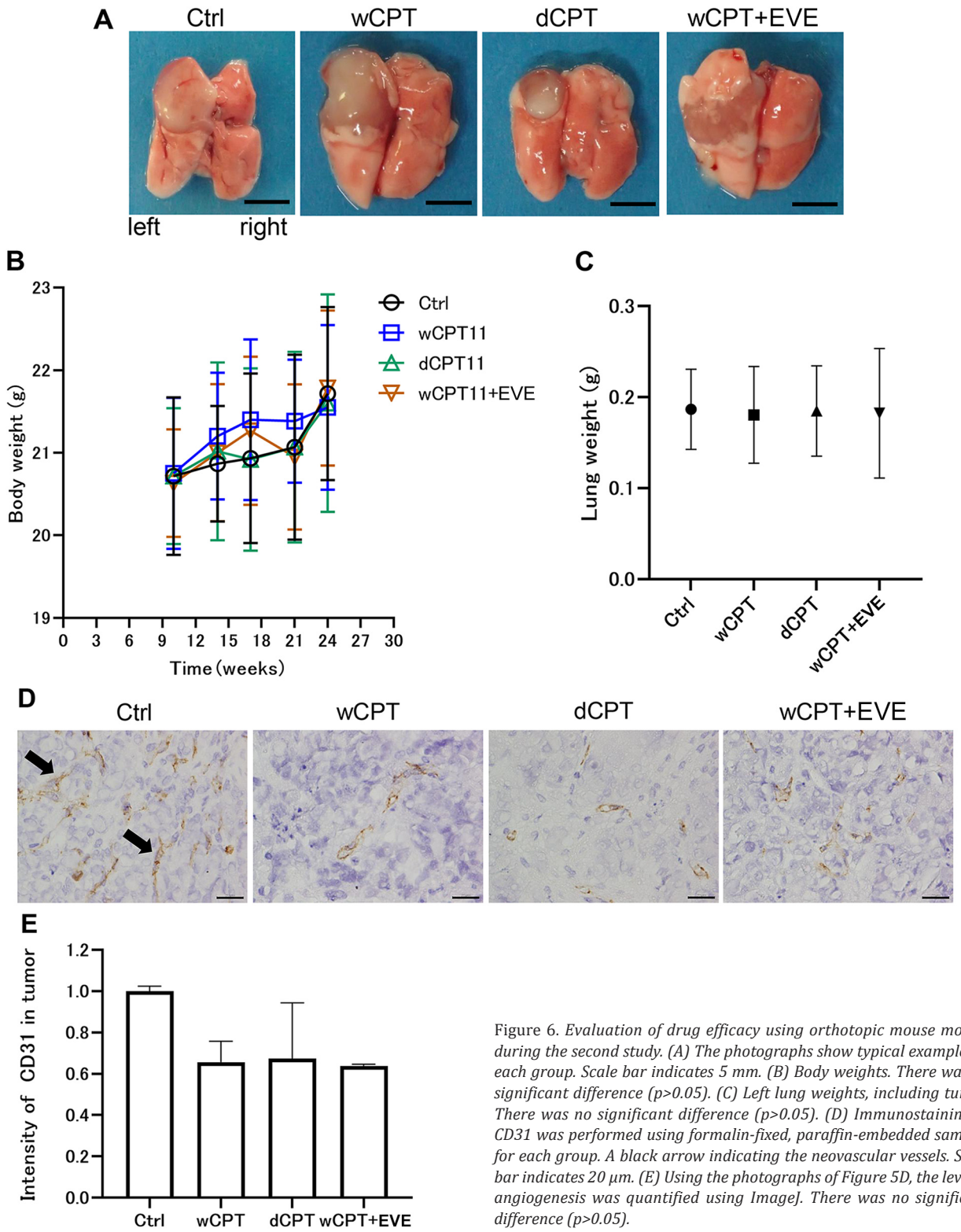

Figure 6. *Evaluation of drug efficacy using orthotopic mouse models during the second study. (A) The photographs show typical examples of each group. Scale bar indicates 5 mm. (B) Body weights. There was no significant difference (p>0.05). (C) Left lung weights, including tumor. There was no significant difference (p>0.05). (D) Immunostaining of CD31 was performed using formalin-fixed, paraffin-embedded samples for each group. A black arrow indicating the neovascular vessels. Scale bar indicates 20 μm. (E) Using the photographs of Figure 5D, the level of angiogenesis was quantified using ImageJ. There was no significant difference (p>0.05).*

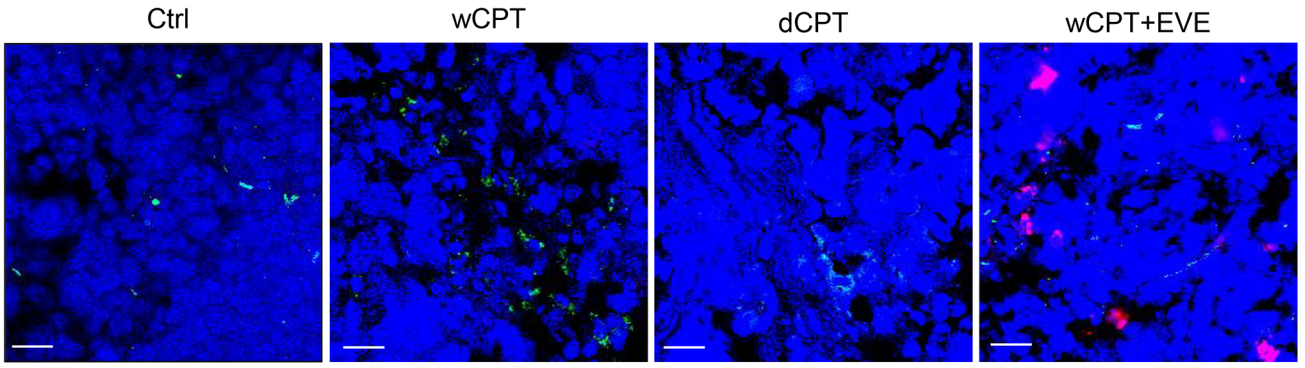

Figure 7. *Immunofluorescence of CD31 and TUNEL. Immunofluorescence of CD31 (green) and TUNEL (magenta). Each image shows the typical example of each group. dCPT-11 was associated with the lowest levels of angiogenesis. There was no apoptosis of tumor blood vessels. Scale bar: 20 μm.*

observed in control or CPT-11 monotherapy groups but was detected in tumors treated with CPT-11 combined with EVE (Figure 7). Vascular apoptosis was not observed.

Discussion

In this study, we demonstrated that daily administration of CPT-11 exerted more pronounced antitumor and anti-angiogenic effects than weekly administration, despite an equivalent cumulative dose intensity. This suggests that treatment scheduling plays a critical role in optimizing therapeutic outcomes for SCLC. Interestingly, VEGFA mRNA expression was not significantly suppressed by CPT-11 *in vitro*, implying that the observed anti-angiogenic effects may be mediated through VEGF-independent pathways, such as endothelial progenitor cell suppression, modulation of thrombospondin-1, or alterations in hypoxia signaling (19, 20). Such mechanisms may involve broader alterations in the tumor microenvironment or alternative signaling pathways that regulate vascular growth (8, 21). Importantly, the temporal pattern observed – angiogenesis inhibition occurring prior to overt tumor shrinkage or apoptosis – supports the hypothesis that suppression of vascular support represents an early and essential step in the therapeutic effect of metronomic chemotherapy. This temporal relationship warrants further mechanistic investigation.

Although EVE did not exhibit strong synergism with CPT-11 in either *in vitro* or *in vivo* settings, a modest reduction in VEGFA expression and induction of tumor apoptosis were observed when combined with CPT-11. These findings suggest that the contribution of EVE may be due more to the promotion of apoptotic responses or modulation of tumor cell survival pathways rather than directly to enhancement of angiogenesis inhibition.

Study limitations. First, the sample size was limited, and quantification of angiogenesis relied primarily on CD31 immunostaining, which may not fully capture functional vascular dynamics. Second, the mechanistic basis for VEGF-independent anti-angiogenic effects remains speculative, and further studies incorporating transcriptomic or proteomic profiling are needed. Finally, translation of these preclinical findings to clinical settings requires careful consideration of pharmacokinetics, tolerability, and patient heterogeneity.

Conclusion

Our results indicate that metronomic CPT-11 exerts antitumor activity at least partly through VEGF-independent suppression of angiogenesis. While the precise molecular mediators remain to be clarified, these findings underscore the importance of exploring non-

VEGF pathways as potential therapeutic targets in SCLC and provide a rationale for future mechanistic studies.

Conflicts of Interest

The Authors have no conflicts of interest to declare in relation to this study.

Authors' Contributions

Yoshihiro Amano: Conceptualization, Formal analysis, Methodology, Project administration, Resources, Visualization, Writing – original draft; Ryosuke Tanino: Resources, Formal analysis, Methodology, Visualization, Writing – review & editing; Rong Sun, Writing – review & editing; Yukari Tsubata: Resources, Writing – review & editing; Takeshi Isobe: Resources, Supervision, Writing – review & editing; Tamio Okimoto: Resources, Supervision, Writing – original draft & editing.

Acknowledgements

The Authors would like to thank Editage (www.editage.jp) for English language editing.

Artificial Intelligence (AI) Disclosure

During the preparation of this manuscript, a large language model (ChatGPT, OpenAI) was used solely for language editing and stylistic improvements in select paragraphs. No sections involving the generation, analysis, or interpretation of research data were produced by generative AI. All scientific content was created and verified by the authors. Furthermore, no figures or visual data were generated or modified using generative AI or machine learning–based image enhancement tools.

References

1 Travis WD: Update on small cell carcinoma and its differentiation from squamous cell carcinoma and other non-small cell carcinomas. Mod Pathol 25 Suppl 1: S18-S30, 2012. DOI: 10.1038/modpathol.2011.150

2 Travis WD, Brambilla E, Burke AP, Marx A, Nicholson AG: Introduction to The 2015 World Health Organization Classification of Tumors of the Lung, Pleura, Thymus, and Heart. J Thorac Oncol 10(9): 1240-1242, 2015. DOI: 10.1097/jto.0000000000000663

3 Vallières E, Shepherd FA, Crowley J, Van Houtte P, Postmus PE, Carney D, Chansky K, Shaikh Z, Goldstraw P: The IASLC Lung Cancer Staging Project: Proposals regarding the relevance of TNM in the pathologic staging of small cell lung cancer in the forthcoming (seventh) edition of the TNM Classification for Lung Cancer. J Thorac Oncol 4(9): 1049-1059, 2009. DOI: 10.1097/JTO.0b013e3181b27799

4 Paz-Ares L, Dvorkin M, Chen Y, Reinmuth N, Hotta K, Trukhin D, Statsenko G, Hochmair MJ, Özgüroğlu M, Ji JH, Voitko O, Poltoratskiy A, Ponce S, Verderame F, Havel L, Bondarenko I, Kazarnowicz A, Losonczy G, Conev NV, Armstrong J, Byrne N, Shire N, Jiang H, Goldman JW, CASPIAN investigators: Durvalumab plus platinum-etoposide versus platinum-etoposide in first-line treatment of extensive-stage small-cell lung cancer (CASPIAN): a randomised, controlled, open-label, phase 3 trial. Lancet 394(10212): 1929-1939, 2019. DOI: 10.1016/s0140-6736(19)32222-6

5 Horn L, Mansfield AS, Szczęsna A, Havel L, Krzakowski M, Hochmair MJ, Huemer F, Losonczy G, Johnson ML, Nishio M, Reck M, Mok T, Lam S, Shames DS, Liu J, Ding B, Lopez-Chavez A, Kabbinavar F, Lin W, Sandler A, Liu SV: First-line atezolizumab plus chemotherapy in extensive-stage small-cell lung cancer. N Engl J Med 379(23): 2220-2229, 2018. DOI: 10.1056/NEJMoa1809064

6 Hashimoto K, Kaira K, Imai H, Miura Y, Shiono A, Mouri A, Yamaguchi OU, Kobayashi K, Kagamu H, Kuji I: Metabolic tumor volume as significant predictor for chemotherapy containing PD-L1 blocker in extensive stage small cell lung cancer. Anticancer Res 44(4): 1541-1551, 2024. DOI: 10.21873/anticanres.16951

7 Wu HL, Zhou HX, Chen LM, Wang SS: Metronomic chemotherapy in cancer treatment: new wine in an old bottle. Theranostics 14(9): 3548-3564, 2024. DOI: 10.7150/thno.95619

8 Simsek C, Esin E, Yalcin S: Metronomic chemotherapy: a systematic review of the literature and clinical experience. J Oncol 2019: 5483791, 2019. DOI: 10.1155/2019/5483791

9 Ogata Y, Mori S, Ishibashi N, Akagi Y, Ushijima M, Murakami H, Fukushima T, Shirouzu K: Metronomic chemotherapy using weekly low-dosage CPT-11 and UFT as postoperative adjuvant therapy in colorectal cancer at high risk to recurrence. J Exp Clin Cancer Res 26(4): 475-482, 2007.

10 Slotkin EK, Meyers PA: Irinotecan dose schedule for the treatment of Ewing sarcoma. Pediatr Blood Cancer 70(1): e30005, 2023. DOI: 10.1002/pbc.30005

11 Salven P, Ruotsalainen T, Mattson K, Joensuu H: High pre-treatment serum level of vascular endothelial growth factor

(VEGF) is associated with poor outcome in small-cell lung cancer. Int J Cancer 79(2): 144-146, 1998. DOI: 10.1002/(sici)1097-0215(19980417)79:2<144::aid-ijc8>3.0.co;2-t

12 Fontanini G, Faviana P, Lucchi M, Boldrini L, Mussi A, Camacci T, Mariani MA, Angeletti CA, Basolo F, Pingitore R: A high vascular count and overexpression of vascular endothelial growth factor are associated with unfavourable prognosis in operated small cell lung carcinoma. Br J Cancer 86(4): 558-563, 2002. DOI: 10.1038/sj.bjc.6600130

13 Sandler A, Gray R, Perry MC, Brahmer J, Schiller JH, Dowlati A, Lilenbaum R, Johnson DH: Paclitaxel–carboplatin alone or with bevacizumab for non–small-cell lung cancer. N Engl J Med 355(24): 2542-2550, 2006. DOI: 10.1056/NEJMoa061884

14 Tiseo M, Boni L, Ambrosio F, Camerini A, Baldini E, Cinieri S, Brighenti M, Zanelli F, Defraia E, Chiari R, Dazzi C, Tibaldi C, Turolla GM, D'Alessandro V, Zilembo N, Trolese AR, Grossi F, Riccardi F, Ardizzoni A: Italian, multicenter, phase III, randomized study of cisplatin plus etoposide with or without bevacizumab as first-line treatment in extensive-disease small-cell lung cancer: The GOIRC-AIFA FARM6PMFJM Trial. J Clin Oncol 35(12): 1281-1287, 2017. DOI: 10.1200/jco.2016.69.4844

15 Alam MM, Fermin JM, Knackstedt M, Noonan MJ, Powell T, Goodreau L, Daniel EK, Rong X, Moore-Medlin T, Khandelwal AR, Nathan CO: Everolimus downregulates STAT3/HIF-1α/VEGF pathway to inhibit angiogenesis and lymphangiogenesis in TP53 mutant head and neck squamous cell carcinoma (HNSCC). Oncotarget 14: 85-95, 2023. DOI: 10.18632/oncotarget.28355

16 Fazio N, Carnaghi C, Buzzoni R, Valle JW, Herbst F, Ridolfi A, Strosberg J, Kulke MH, Pavel ME, Yao JC: Relationship between metabolic toxicity and efficacy of everolimus in patients with neuroendocrine tumors: A pooled analysis from the randomized, phase 3 RADIANT-3 and RADIANT-4 trials. Cancer 127(15): 2674-2682, 2021. DOI: 10.1002/cncr.33540

17 Sun JM, Kim JR, Do IG, Lee SY, Lee J, Choi YL, Ahn JS, Ahn MJ, Park K: A phase-1b study of everolimus plus paclitaxel in patients with small-cell lung cancer. Br J Cancer 109(6): 1482-1487, 2013. DOI: 10.1038/bjc.2013.467

18 Isobe T, Onn A, Morgensztern D, Jacoby JJ, Wu W, Shintani T, Itasaka S, Shibuya K, Koo PJ, O'Reilly MS, Herbst RS: Evaluation of novel orthotopic nude mouse models for human small-cell lung cancer. J Thorac Oncol 8(2): 140-146, 2013. DOI: 10.1097/JTO.0b013e3182725ff9

19 Murakami H, Ogata Y, Akagi Y, Ishibashi N, Shirouzu K: Circulating endothelial progenitor cells in metronomic chemotherapy using irinotecan and/or bevacizumab for colon carcinoma: Study of their clinical significance. Exp Ther Med 2(4): 595-600, 2011. DOI: 10.3892/etm.2011.253

20 Bocci G, Francia G, Man S, Lawler J, Kerbel RS: Thrombospondin 1, a mediator of the antiangiogenic effects of low-dose metronomic chemotherapy. Proc Natl Acad Sci USA 100(22): 12917-12922, 2003. DOI: 10.1073/pnas.2135406100

21 Kerbel RS, Kamen BA: The anti-angiogenic basis of metronomic chemotherapy. Nat Rev Cancer 4(6): 423-436, 2004. DOI: 10.1038/nrc1369